Journal of Computational Acoustics, Vol. 10, No. 4 (2002) 445–464

PROPELLER NOISE FROM A LIGHT AIRCRAFT FOR LOW-FREQUENCY MEASUREMENTS OF THE SPEED OF SOUND IN A MARINE SEDIMENT

MICHAEL J. BUCKINGHAM*, ERIC M. GIDDENS,
FERNANDO SIMONET and THOMAS R. HAHN

Marine Physical Laboratory, Scripps Institution of Oceanography, University of California, San Diego, 8820 Shellback Way, La Jolla, CA 92093-0238, USA

Received 30 August 2002
Revised 30 August 2002

The sound from a light aircraft in flight is generated primarily by the propeller, which produces a sequence of harmonics in the frequency band between about 80 Hz and 1 kHz. Such an airborne sound source has potential in underwater acoustics applications, including inversion procedures for determining the wave properties of marine sediments. A series of experiments has recently been performed off the coast of La Jolla, California, in which a light aircraft was flown over a sensor station located in a shallow (approximately 15 m deep) ocean channel. The sound from the aircraft was monitored with a microphone above the sea surface, a vertical array of eight hydrophones in the water column, and two sensors, a hydrophone and a bender intended for detecting shear waves, buried 75 cm deep in the very-fine-sand sediment. The propeller harmonics were detected on all the sensors, although the *s*-wave was masked by the *p*-wave on the buried bender. Significant Doppler shifts of the order of 17%, were observed on the microphone as the aircraft approached and departed from the sensor station. Doppler shifting was also evident in the hydrophone data from the water column and the sediment, but to a lesser extent than in the atmosphere. The magnitude of the Doppler shift depends on the local speed of sound in the medium in which the sensor is located. A technique is described in which the Doppler difference frequency between aircraft approach and departure is used to determine the speed of sound at low-frequencies (80 Hz to 1 kHz) in each of the three environments, the atmosphere, the ocean and the sediment. Several experimental results are presented, including the speed of sound in the very fine sand sediment at a nominal frequency of 600 Hz, which was found from the Doppler difference frequency of the seventh propeller harmonic to be 1617 m/s.

Keywords: Marine sediments; dispersion; attenuation; doppler; propeller noise; aircraft sound.

1. Introduction

Throughout the past half-century, considerable efforts have been made to measure the properties of compressional (sound) and transverse (shear) waves in marine sediments. Hamilton's

*Also affiliated to: Institute of Sound and Vibration Research, The University, Southampton SO17 1BJ, England.

contributions to this enterprise deserve special mention, since he not only collected and published many data sets of unsurpassed quality on the properties of waves in sediments, but he also developed an empirical, visco-elastic model of wave propagation in a porous medium which accurately represents the data. References to many of his papers can be found in the bibliography of Hamilton's final review paper on the acoustic properties of sediments.[1]

More recently, the Office of Naval Research launched a research initiative on the interaction of high-frequency sound with marine sediments, an integral part of which was the Sediment Acoustics Experiment 1999 (SAX99).[2,3] This multidisciplinary experiment was performed from late September to mid November 1999 in the northeastern Gulf of Mexico, at a site 2 km off Fort Walton Beach, Florida, where the water is 18–19 m deep. An important objective of SAX99 was to characterize the physical and wave properties of the sediment at the site, which consists of a well-sorted medium sand with a mean grain diameter of 420 μm and a fractional porosity $N \approx 0.38$. Using *in-situ* probes and a time-of-flight technique,[4] the speed of sound in the SAX99 sediment was found to be approximately 1780 m/s at a frequency of 38 kHz. Between 25 and 100 kHz, the speed of sound showed weak frequency dispersion, the trend being a positive gradient of the order of 1% per decade of frequency.

The degree of dispersion is one of the factors that can be used to distinguish between theoretical models of wave propagation in a saturated granular medium such as a marine sediment. In particular, the Biot model,[5,6] which is based on the viscous flow of pore fluid between the mineral grains, predicts relatively strong dispersion with a positive gradient in the frequency band between 1 and 2 kHz, whereas, in the same frequency range, Buckingham's inter-granular sliding theory[7] yields weaker dispersion, of the order of 1% per decade of frequency. According to both theories, in the limit of low frequency, the speed of sound in the material takes the value given by Wood's equation[8] for a two-phase medium. Such behavior implies that, in the presence of a sufficiently slow disturbance, the mineral grains act as though they were in suspension with negligible grain-to-grain interaction.

As a test of the theoretical predictions, it would be desirable to have an *in-situ* measure of the low-frequency (< 2 kHz) sound speed in marine sediments. In view of the success of time-of-flight measurements at frequencies of several tens of kHz, a similar approach at lower frequencies would seem to hold some promise. In the lower frequency ranges, however, the longer wavelengths dictate a greater source-to-receiver separation, of the order of 10 m or more, which, in addition to problems of implementation, introduces difficulties associated with reflections from the seawater-sediment interface. Moreover, marine sediments often lack homogeneity over such distances due to inclusions such as shells and shell fragments.

An alternative to travel-time techniques for making *in-situ* measurements of the speed of sound in a marine sediment is discussed in this paper. In essence, the method relies on just a single hydrophone buried in the sediment, which records the low-frequency (<1 kHz) sound from a single-engine, propeller-driven, light aircraft as it overflies the sensor station. The Doppler shifts on the approach to and departure from the sensor station provide a direct measure of the local speed of sound in the sediment. Since flying machines are rarely used in underwater acoustics applications, we begin with a brief introductory discussion of the major sources of sound emitted by a light aircraft.

2. Sources of Sound from a Propeller-Driven Aircraft

In most single-engine light aircraft, the power plant is a four-stroke reciprocating engine with a direct drive to a propeller, which in cruising flight turns typically at about 2500 rpm. (A few of the smaller engines operate at increased rpm and drive the propeller through a reduction gear.) Both the engine and propeller produce sounds which are periodic, since they originate in mechanical rotation mechanisms, but as these pressure waveforms are not purely sinusoidal, their spectra contain a fundamental frequency plus higher-order Fourier components, or harmonics, at multiples of the fundamental. The frequency of the first harmonic, that is the fundamental, is between 50 and 100 Hz, depending on rpm, and as many as a dozen higher harmonics may be detectable up to about 1 kHz.

The principal source of engine sound is the regular firing of the cylinders. The fundamental frequency of this mechanism is given by the expression

$$f_{\text{eng}} = \frac{NR}{60P}\,, \tag{2.1}$$

where N is the number of cylinders, R is the rpm, and P is the number of revolutions per firing per cylinder. In a four-stroke engine, the crankshaft rotates twice for each cylinder firing, that is $P = 2$. For such an engine with four cylinders ($N = 4$) and operating at $R = 2500$ rpm, the frequency of the fundamental tone is 83.3 Hz, with harmonics at 166.6 Hz, 250 Hz, 333.3 Hz, ...

In flight the primary source of sound from a light aircraft is not the engine but the propeller, which continuously parts the air in a regular, cyclic fashion with respect to a stationary observer. As discussed by Goldstein,[9] a theoretical description of the far-field pressure from an aircraft propeller was developed by Gutin,[10] whose theory was subsequently extended to include near-field effects.[11] At high blade speeds, the dominant sound from the propeller, generated mainly at the tips, is often referred to as "thickness" noise.[12] The fundamental frequency of propeller noise is

$$f_{\text{prop}} = \frac{BR}{60}\,, \tag{2.2}$$

where B is the number of blades. Assuming a direct drive to a two-bladed propeller ($B = 2$) rotating at $R = 2500$ rpm, the frequency of the fundamental is 83.3 Hz, with harmonics at multiples of the fundamental.

According to Eqs. (2.1) and (2.2), the engine and propeller harmonics are identical for the particular combination of a four-cylinder engine driving a two-bladed propeller. In general, the engine and propeller harmonics are not the same, as may be verified by considering a six-cylinder engine driving a two-bladed propeller or a four-cylinder engine driving a three-bladed propeller. A more complete discussion of propeller noise, including examples of spectra showing the prominent harmonics, can be found in the paper by Magliozzi *et al.*[13] These authors also point out that the radiation pattern of the noise from the propeller is not omni-directional: in the absence of unsteady forces, propeller noise is axisymmetric, with a main lobe near the plane of rotation when the aircraft is stationary. In flight, with a steady

aerodynamic flow in the axial direction, the main lobe tends to be pushed back about 20° behind the plane of the propeller.[9]

A third source of sound from an aircraft in flight, in addition to the engine and the propeller, is the airframe,[12] which, as discussed by Crighton,[14] became of some concern in the 1970s and 1980s in connection with quietening programmes for commercial jet transports. Airframe noise, which arises from turbulent aerodynamic flow over landing gear, flaps and lifting surfaces, is usually significant only during certain phases of flight, notably the approach to landing. Even then its main effect is on observers within the aircraft rather than those on the ground below. Since a light aircraft participating in underwater acoustics experiments is unlikely to be in the landing configuration, airframe noise as a potential source of exploitable sound is discounted.

Of the remaining two sources, the propeller predominates over the engine as the main generator of light-aircraft noise when the aircraft is in flight. Since the propeller produces a comb of very narrow band tones between 50 Hz and 1 kHz, a light aircraft would seem to have the potential to act as a low-frequency sound source in underwater acoustics applications. One such application is the measurement of the speed of sound in marine sediments over the low frequency range where dispersion is of interest in connection with testing the various theoretical predictions. To explore the possibilities offered by a light aircraft for ocean-acoustics research, a series of experiments has recently been conducted at SIO with a

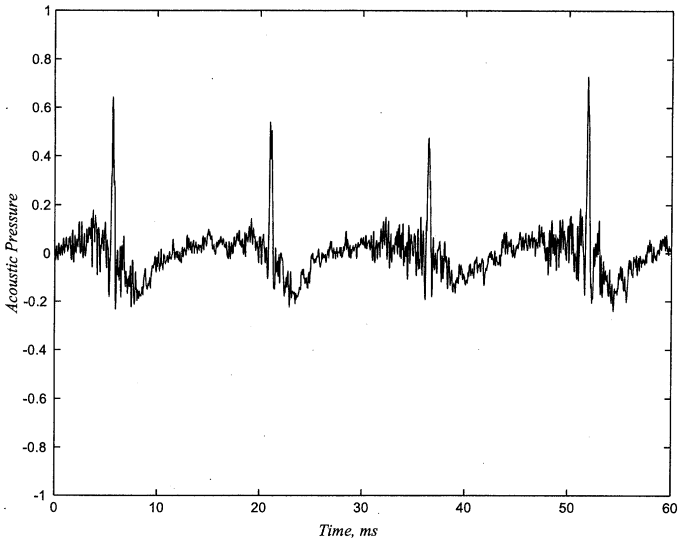

(a)

Fig. 1. Acoustic signature of the Tobago recorded using a wing-tip microphone on 26 May 2002 with the aircraft stationary on the ground and the engine operating at 2000 rpm. (a) Pressure time series (uncalibrated) showing the periodic structure of the sound, including regular spikes at the cylinder firing rate. (b) Normalized (to the first peak) pressure power spectrum showing a sequence of sharp principal maxima, which are propeller harmonics. The spectral resolution of the plot is 1.3 Hz.

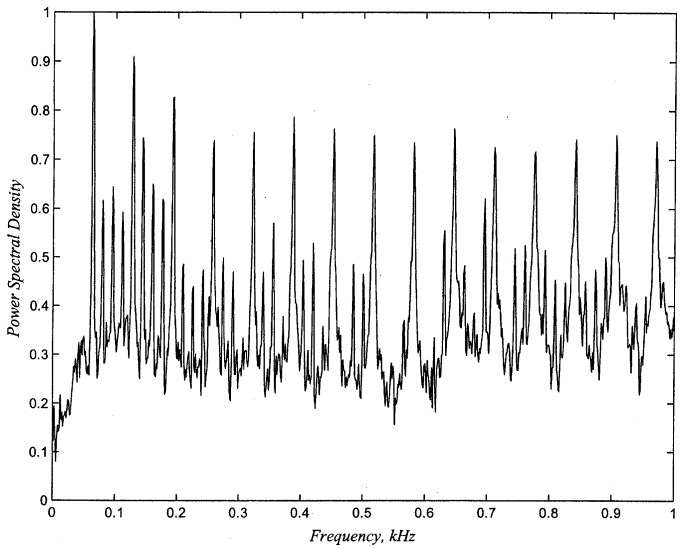

(b)

Fig. 1. (*Continued*)

low-wing, four-seat, single-engine aeroplane, a Socata Tobago TB10, which has a four-cylinder, 180 hp Lycoming engine driving a two-bladed propeller.

As described in subsequent sections, the sound from the Tobago has been recorded with the aircraft in flight over the ocean at altitudes between 33 m and 330 m. For reference, a ground-based measurement with the Tobago stationary has also been performed, using a microphone at the port wing-tip, about 4 m from the spinner, 1 m above the ground and approximately 20° behind the plane of the propeller. A representative example of the observed pressure waveform is shown in Fig. 1(a) with its power spectrum in Fig. 1(b), the latter illustrating nicely the prominent harmonic structure (the sequence of principal maxima) of the radiated sound. Notice also the smaller peaks appearing in groups of three between the principal maxima, which are secondary or sub-harmonics due to the unequal heights of the four cylinder-firing-rate spikes in the time series (Fig. 1(a)). These spikes are not identical in amplitude because of slight differences between the four cylinders, which gives rise to the three equi-spaced sub-harmonics between the main harmonics in Fig. 1(b).

3. Over-Ocean Flying Experiments

Between 3 March and 5 July 2002, five over-ocean experiments were conducted in which the sound from the Tobago was monitored with acoustic sensors located in the atmosphere, the water column and the sediment. Each of the five flights lasted about 1.5 h from take-off to touch down, with 1 h or so on station. Two sensor stations were used in the experiments, both of which were located approximately 1.5 km north-west of Scripps pier, La Jolla, California, where the water is shallow and the sediment is a very fine sand that is essentially free of

inclusions, such as shell fragments, that would act as acoustic scatterers. For convenience, the two sensor stations are designated A (32° 53.8′ N, 117° 16.1′ W; water depth, $d = 20$ m) and B (32° 53.889′ N, 117° 15.718′ W; water depth, $d = 15$ m).

The most comprehensively instrumented station was B, as illustrated in Fig. 2. The sound of the aircraft was monitored in the atmosphere, with a microphone about 1 m above the sea surface; in the water, with a vertical array of eight hydrophones; and in the sediment, where a hydrophone and a shear-wave sensor (a bender) were buried at a depth of about 75 cm. The buried sensors, which were jetted into the sediment by divers over a week before being used for making measurements, were part of an effort to detect the *p*-wave and *s*-wave (if present) produced in the sediment by the propeller noise from the aircraft. The bender was aligned as closely as possible with the aircraft track in order to maximize its response to the *s*-wave, but no evidence for the existence of an aircraft-generated shear wave has so far been found in the bender data. In fact, the bender output was dominated by the *p*-wave, suggesting that the alignment of the shear sensor with the aircraft track was less than perfect. This is a tricky problem to solve, since the orientation was set by divers at the time of burial, using a magnetic compass to align the principal plane of the bender with the aircraft track, which itself was somewhat variable because of winds and slight inconsistencies in flight performance.

Aircraft navigation, sensor positioning and timing were performed using handheld GPS receivers. The GPS receiver used in the aircraft has a built-in pressure sensor that was calibrated before flight at a known elevation to provide accurate altimetry information.

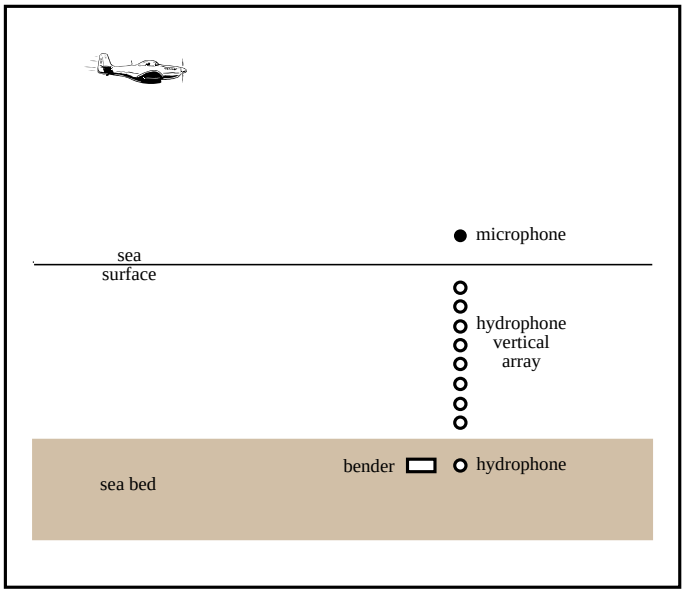

Fig. 2. Schematic of sensor configuration at station B for the experiment of 2 July 2002. The buried bender and hydrophone were 75 cm beneath the seawater-sediment interface and the microphone was 1 m above the sea surface.

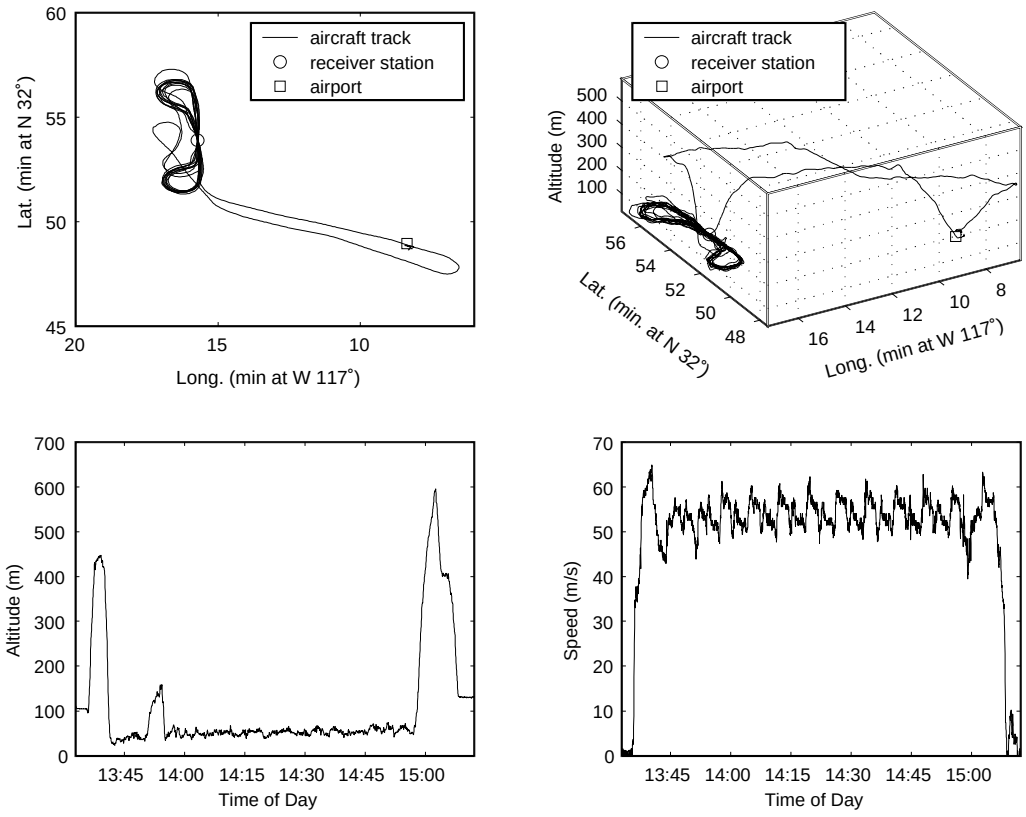

Fig. 3. GPS flight data for the experiment of 2 July 2002. Clockwise from top left, the panels show lateral position, 3-D track, ground speed versus time and altitude versus time. Total flight time from take-off to landing was 1.7 hours.

Thus, GPS records of the 3-D track and the elevation of each flight are available, in addition to lateral position and ground speed, as exemplified in Fig. 3 for the flight of 2 July. On this occasion, over twenty overflights of the sensor station were made at a nominally uniform altitude of 66 m on headings of 150° and its reciprocal 330°. These tracks are about 1 km offshore and approximately parallel to the cliffs north of Scripps pier. Typical flight parameters for all the experiments were: airspeed of 106 knots (53 m/s); engine speed 2500 rpm; and altitude 66 m, although in some of the flights the altitude was varied in increments of 33 m between 33 m and 330 m. Notice that the ground speed shown in the bottom right panel of Fig. 3 exhibits regular fluctuations even though the airspeed was held constant: an onshore breeze of about 10 knots (5 m/s) was blowing, which accounts for the variations.

4. Doppler Signatures of Overflight on 2 July 2002

Figure 4 shows calibrated spectrograms of the propeller noise, as monitored in the air, water and sediment, during an overflight of sensor station B by the Tobago on 2 July 2002. The time window in each of the panels is centred on the moment the aircraft was directly

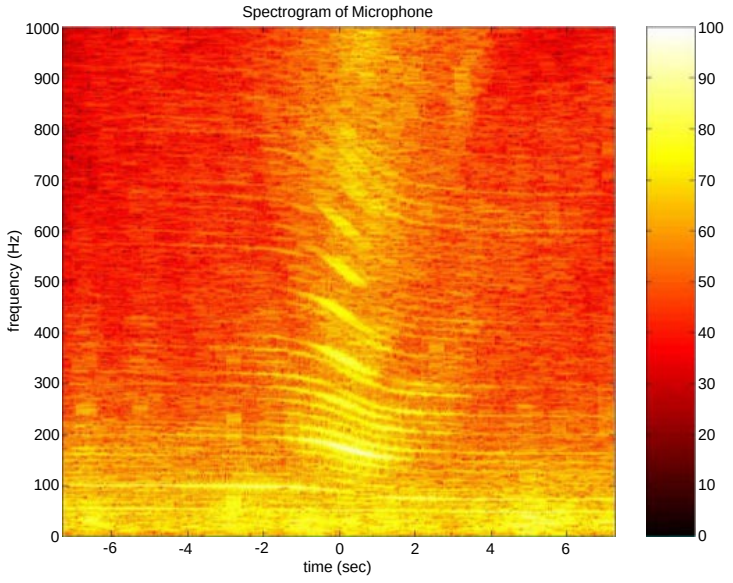

(a)

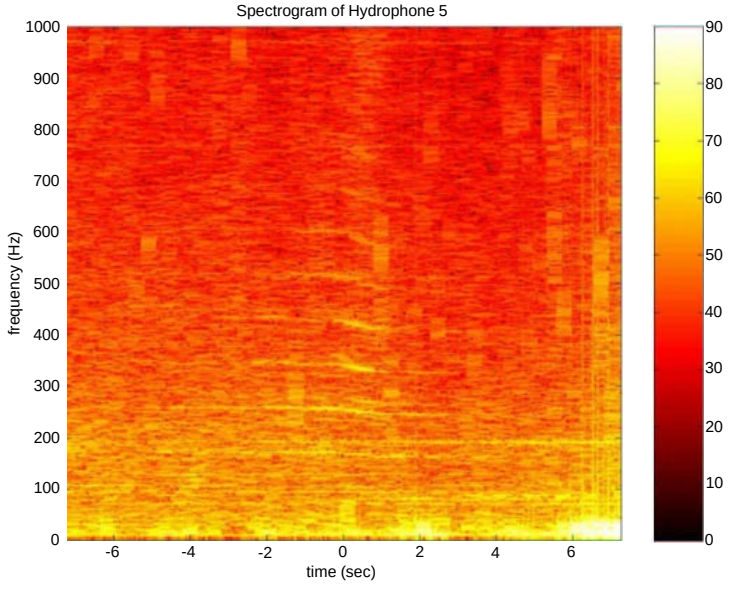

(b)

Fig. 4. Calibrated spectrograms of the propeller noise from an overflight of the Tobago at an altitude of 66 m, speed of 53 m/s and engine operating at 2500 rpm on 2 July 2002. The spectral resolution is 2.44 Hz and the colour bars are in dB re 1 μPa^2/Hz. (a) Airborne sound recorded on microphone 1 m above the sea surface, (b) water-borne sound recorded on hydrophone at depth of 10 m and (c) sediment sound recorded on hydrophone buried at depth of 75 cm beneath seafloor. The water depth at the sensor station is $d \approx 15$ m.

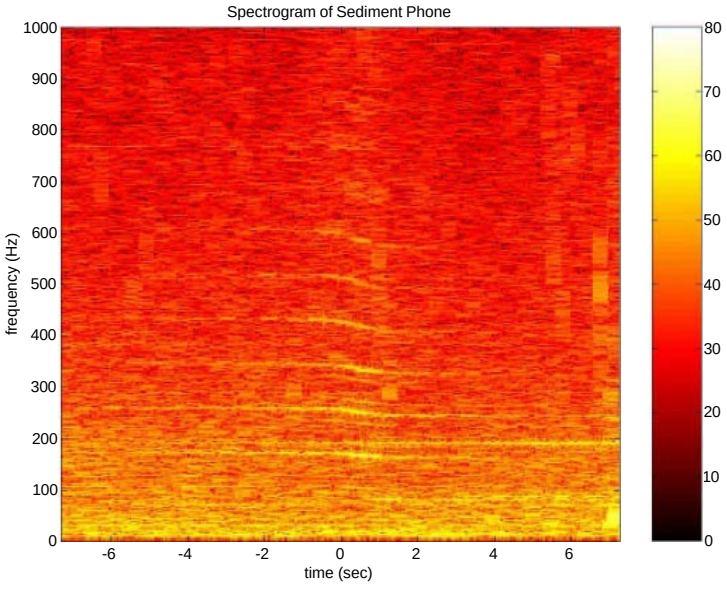

(c)

Fig. 4. (*Continued*)

overhead, that is, at the closest point of approach (CPA). Not surprisingly, the harmonic structure of the propeller noise was easily detectable on the microphone just above the sea surface (Fig. 4(a)). The frequency of each harmonic can be seen to exhibit a significant Doppler upshift on the approach to and downshift on the departure from the sensor station. These Doppler shifts, which amount to about 17% of the intrinsic (unshifted) frequency, are consistent with the ratio of the aircraft speed ($\approx$ 53 m/s) to the sound speed in air ($\approx$ 340 m/s). Notice that the harmonics observed when the aircraft is in flight attenuate more rapidly with increasing frequency than those in Fig. 1(b), which were observed at close range with the aircraft stationary on the ground. Acoustic attenuation in the atmosphere is responsible for the fading of the higher harmonics in Fig. 4(a).

Assuming a smooth sea surface, a critical angle exists at the atmosphere-ocean interface of approximately 13°. An acoustic ray from the aircraft that is steeper than the critical angle will be refracted into the ocean where it should be detectable on a submerged hydrophone. Indeed, several observations of sound transmission into the ocean from an overflying aircraft have appeared in the literature. One of the early reports was by Urick,[15] who recorded the sub-surface sound from a U.S. Navy P3C (four engine turbo-prop) aircraft flying at a speed of 200 knots ($\approx$ 100 m/s) at altitudes of 77, 154 and 308 m; and Richardson *et al.*[16] present the observed sub-surface acoustic spectra of two twin-engine aircraft, a deHavilland Twin Otter flying at a speed of 44 m/s and an altitude of 460 m, and a Britten Norman Islander at an altitude of 610 m. Medwin *et al.*[17] investigated the spectral characteristics of sound transmitted through a rough sea surface from a Sikorsky SH-3D helicopter at various low (few hundred metre) altitudes, both in the hover and moving at slow speed.

It is evident in Fig. 4(b) that we too could detect underwater sound from the aeroplane as it flew overhead. The hydrophones in the water column all registered clear signals for several seconds on either side of the CPA. Like the airborne arrivals, the underwater signals are Doppler shifted, upwards on approach and downwards on departure, but the magnitude of the shift is considerably less than that in air. As discussed in more detail later, the reduced Doppler shift in the underwater signals arises directly from the fact that the speed of sound is higher in water, by a factor of about five, than in air.

As far as we are aware, the sound from an aircraft has not previously been detected in a marine sediment. Figure 4(c) shows that, in our experiments, some of the acoustic energy from the Tobago propagated through the water column and into the sediment, and was detectable on the buried hydrophone for several seconds on either side of the CPA. On the approach and departure, Doppler upshifts and downshifts, respectively, are visible on the harmonics and, since the buried phone is in a static environment (unlike the phones in the water column, which may be subject to the effects of hydrodynamic flow), these shifted tones tend to be very stable. As with the water-borne arrivals, the harmonics in the sediment signal are Doppler shifted to a considerably lesser extent than those in the atmosphere, again because of the higher sound speed in the local medium, that is, the very fine sand comprising the sea bed.

The presence of detectable acoustic signals in the air, water and sediment suggests that low-frequency sound from a light aircraft may hold some promise for underwater acoustics applications. From the simple observation that the local environment (air, water or sediment) modifies the magnitude of the Doppler shifts on the propeller harmonics, it would seem that the received sound contains useful information on the acoustic properties of the medium immediately surrounding the sensor.

Obviously, the speed of the aircraft is considerably greater than that of most acoustic sources used in low-frequency, underwater acoustics applications, resulting in Doppler shifts that are also relatively high. These large Doppler shifts perhaps constitute the main distinguishing factor between an aircraft sound source and other more conventional sources. In the following discussion, the Doppler shifts on the harmonics in the acoustic signature of the propeller are examined in a little more detail, with a view to illustrating how an aeroplane may be used to quantify the speed of sound in a marine sediment.

5. Doppler Shifts and Local Sound Speed

Consider an aircraft sound source flying straight and level above the horizontally stratified ocean environment sketched in Fig. 5. For simplicity the sound speed is assumed to be constant in the atmosphere, the ocean and the sediment, but if this condition were relaxed, the same basic ideas would still apply. An acoustic ray launched from the aircraft is refracted from the atmosphere into the water column and from there into the sediment, where, in the interest of being specific, the speed of sound is assumed to be higher than in sea water. Imagine sensors located as indicated at three points along the ray, one in the air (medium 1), one in the water (medium 2) and one in the sediment (medium 3). The Doppler shift observed

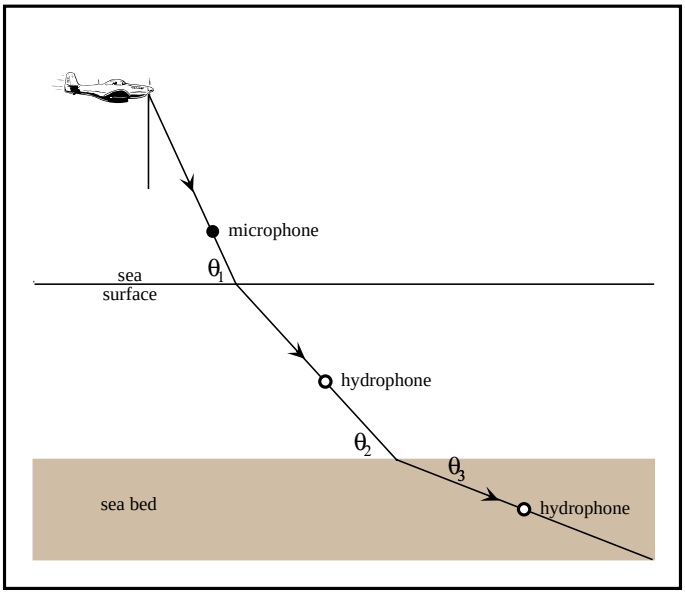

Fig. 5. Schematic showing refraction of a ray through a three layered, horizontally stratified environment.

at each of the sensors will be the same, since the frequency of the ray does not change as it crosses from one medium to another. If the trajectory of the aircraft is in the same vertical plane as the sensors, as depicted in Fig. 5, the Doppler shifted frequency f_D is given by the expression[18,19]

$$f_D(\theta_i) = \frac{f}{1 - \dfrac{v}{c_i}\cos\,\theta_i}\,, \quad i = 1,\, 2,\, 3\,, \tag{5.1}$$

where f may be thought of as the intrinsic frequency of one of the propeller harmonics, v is the speed of the aircraft in the horizontal, c_i is the sound speed in medium $i = 1$, 2 or 3, and θ_i are the corresponding three angles of elevation *at the time of transmission*. Since Snell's law states that $[\cos\,\theta_i]/c_i$ remains constant as the ray is refracted at the boundaries, it is evident that f_D conforms with the requirement that the frequency should be invariant along the propagation path through the three media. Figure 6(a) shows the Doppler frequency from Eq. (5.1) plotted as a function of the elevation angle in air.

When the aircraft is at long range from the sensor station, the angle of elevation in all three media takes the limiting values of 0 (on approach) and π (on departure). If, for a given harmonic, Δ_i denotes the difference between the up-shifted and down-shifted Doppler frequencies at the two limiting ranges, then from Eq. (5.1)

$$\Delta_i \equiv f_D(0) - f_D(\pi) = \frac{2\bar{f}_i^{\,2} v}{f c_i} \approx \frac{2fv}{c_i}\,, \tag{5.2}$$

where

$$\bar{f}_i = \sqrt{f_D(0) f_D(\pi)} \tag{5.3}$$

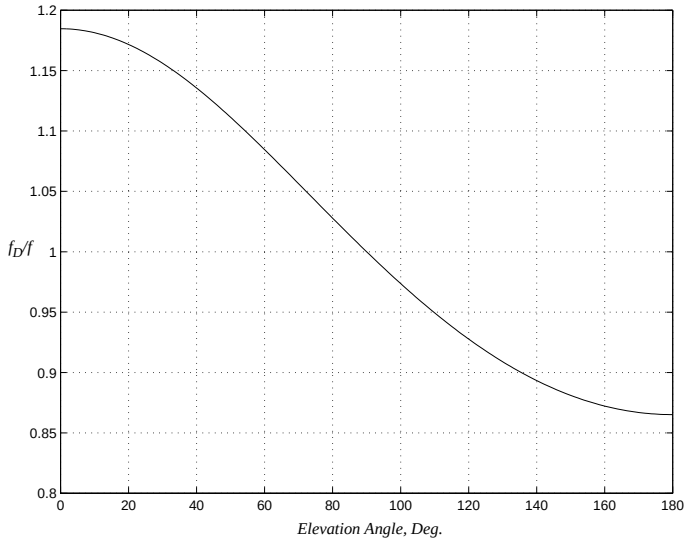

(a)

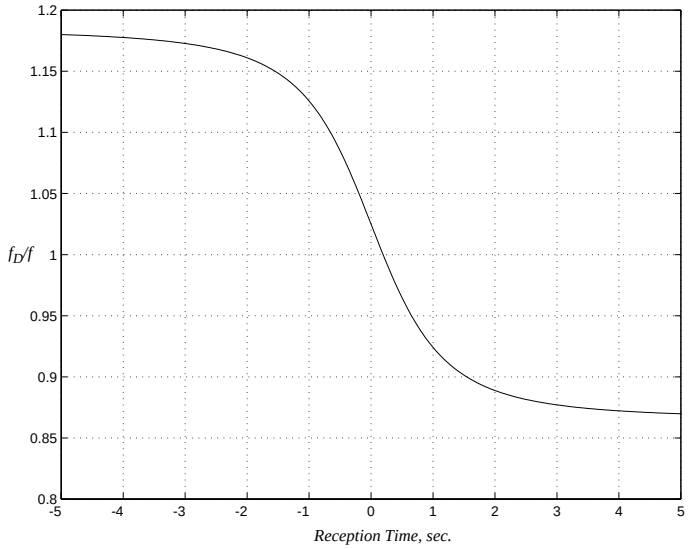

(b)

Fig. 6. Doppler shifted frequency (normalized to the intrinsic frequency) as a function of (a) elevation angle above the microphone at time of transmission [Eq. (5.1)] and (b) time of reception at the microphone [Eq. (5.5)]. Parameter values: $M = 0.1559$ and $h = 66$ m.

is the geometric mean of the limiting up- and down-shifted frequencies and the approximation in Eq. (5.2) follows from setting $\bar{f}_i \approx f$.

The simple result in Eq. (5.2) states that the difference frequency, Δ_i, scales inversely with the local speed of sound, c_i. This accounts for the fact that, in the spectrograms of

Fig. 4, the difference frequency in air is greater than that in water by a factor of approximately five, which is just the ratio of the sound speeds in the two media. The converse of Eq. (5.2) is that the local speed of sound is inversely proportional to the difference frequency. This suggests that a measurement of the difference frequency on a single hydrophone buried in the sediment may be used to estimate the speed of sound in the porous medium over the frequency band of the propeller harmonics. The constant of proportionality linking the difference frequency to the speed of sound involves parameters that are not difficult to measure: the intrinsic frequency of a harmonic, f; the speed of the aircraft, v; and the geometric mean of the limiting values of the up- and down-shifted frequencies, $\bar{f}_3$.

It is clear from Eq. (5.2) that the speed of sound in the sediment can be expressed in several ways:

$$c_3 = \frac{2\bar{f}_3^2 v}{f\Delta_3} \tag{5.4a}$$

$$= \frac{\bar{f}_3^2 \Delta_2}{\bar{f}_2^2 \Delta_3} c_2 \tag{5.4b}$$

$$= \frac{\bar{f}_3^2 \Delta_1}{\bar{f}_1^2 \Delta_3} c_1 \tag{5.4c}$$

Assuming that the speed of sound in air (c_1) and sea water (c_2) are known and that the Doppler frequencies at long range can be measured in each of the three media, these three expressions provide considerable redundancy in the estimation of the speed of sound in the sediment (c_3). There is further redundancy in the fact that the speed of the aircraft, v, appearing in Eq. (5.4a) is available from the GPS record but may also be accurately estimated by fitting an expression such as Eq. (5.1) to the full set of Doppler shifted harmonics observed on the microphone in air.

However, for the purpose of such a curve fit, it is more convenient to work in terms of the *time of reception*, t, (since it is arrival time that is recorded in most measurements) rather than θ_1, which is the angle of elevation of the aircraft at the *time of transmission*. With a little algebra, the expression in Eq. (5.1) for the Doppler shifted frequency may be modified to become

$$f_D = \frac{f}{(1-M^2)} \left[1 - \frac{Mvt}{\sqrt{(vt)^2 + (1-M^2)h^2}} \right] , \tag{5.5}$$

where $M = v/c_1$ is the Mach number of the aircraft, h is the altitude, and $t = 0$ is the time at which the aircraft is directly above the receiver. Although the zero-Doppler signal is transmitted when the aircraft is overhead at time $t = 0$, there is a travel-time delay before arrival at the microphone, which from Eq. (5.7) is given by

$$t_0 = \frac{Mh}{v} = \frac{h}{c_1} . \tag{5.6}$$

This delay, of course, is just the time taken for the acoustic signal to travel vertically downwards from the aircraft to the microphone. Using the flight parameters appropriate to the spectrograms in Fig. 4, the zero-Doppler delay takes the value $t_0 = 194$ ms.

In Fig. 6(b), the Doppler-shifted frequency given by Eq. (5.5) is plotted as a function of reception time t with $M = 0.1559$ and $h = 66$ m. A direct comparison with the spectrogram in Fig. 4(a) is now possible, from which it is evident that Eq. (5.5) follows the shape of the measured airborne harmonics satisfactorily. In general, by fitting Eq. (5.5) to measurements of airborne harmonics such as those shown in Fig. 4(a), the speed of the aircraft may be estimated and, as a bonus, the altitude h is also returned.

6. Preliminary Estimates of Sound Speed

It is clear that, with an aircraft as a sound source, the speed of sound in the three media, air, sea water and sediment, may be estimated from the Doppler-shift data in several different ways. A further advantage of the aircraft is that tracks can be repeatedly flown over the sensor station, to build up a large data set which can be heavily averaged, thereby reducing measurement errors arising from fluctuations in airspeed, wind vector and other variables in the experimental procedure.

As a preliminary to such a statistical analysis, consider just one overflight, say the flight that produced the three spectrograms in Fig. 4, and suppose that the Doppler shifts in only a single harmonic are used to evaluate the speed of sound in air, sea water and sediment from Eq. (5.2) (actually, its converse). The sole purpose of this exercise is to demonstrate that the Doppler-shifted harmonics return local sound speeds of the correct order of magnitude. It should be borne in mind that the resultant sound speeds will involve measurement errors, the magnitudes of which have not been estimated, but which could be significantly reduced by averaging. The Doppler-difference frequency, being the relatively small difference between two larger numbers, is particularly susceptible to error. This difficulty is reduced by working with higher-order harmonics. In all the estimates, the speed of the aircraft is taken to be $v = 53$ m/s and the intrinsic frequency is approximated by the geometric mean in Eq. (5.3).

Taking the seventh harmonic in each of the spectrograms of Fig. 4, the Doppler shifted frequencies on approach and departure are identified visually. For the microphone data in Fig. 4(a), the up- and down-shifted Doppler frequencies are 696.6 and 507.7 Hz, respectively, which yield a speed of sound in air of $c_1 \approx 334$ m/s. The corresponding frequencies for the sea water data in Fig. 4(b) are 612 and 571 Hz, which return a sound speed in the water of $c_2 \approx 1527$ m/s. Finally, the respective frequencies in the sea bed data of Fig. 4(c) are 606 and 568, Hz, from which the sound speed in the very-fine-sand sediment off Scripps pier is estimated to be $c_3 \approx 1617$ m/s.

The estimate of 334 m/s for the speed of sound in air is about 6 m/s below the value expected for the atmospheric conditions of the day (air temperature of approximately 18°C), a small discrepancy which is attributed to a combination of factors, including a breeze of a few m/s and an imperfect estimate of the Doppler difference frequency. The latter error is largely due to the somewhat coarse resolution of the spectrograms (2.44 Hz), which will

be improved in future processing. At 1527 m/s, the estimate of the speed of sound in sea water is a little higher than the value of 1515 m/s that was measured at the depth of the hydrophone ($d = 10$ m) during the experiment using a Sea-Bird temperature profiler (Fig. 7). Again, this error is mainly an effect of the frequency cell width on the estimate of the Doppler difference frequency. For the sediment, the estimated value of 1617 m/s compares reasonably with previously reported measurements of the speed of sound in very fine sand, which are spread between about 1610 and 1720 m/s, as summarized in Fig. 8 of Buckingham.[20] It should be appreciated that these earlier measurements in very fine sand, by various investigators including Hamilton[21,22] and Richardson,[23,24] were all performed at considerably higher frequencies than the nominal 600 Hz of the seventh propeller harmonic.

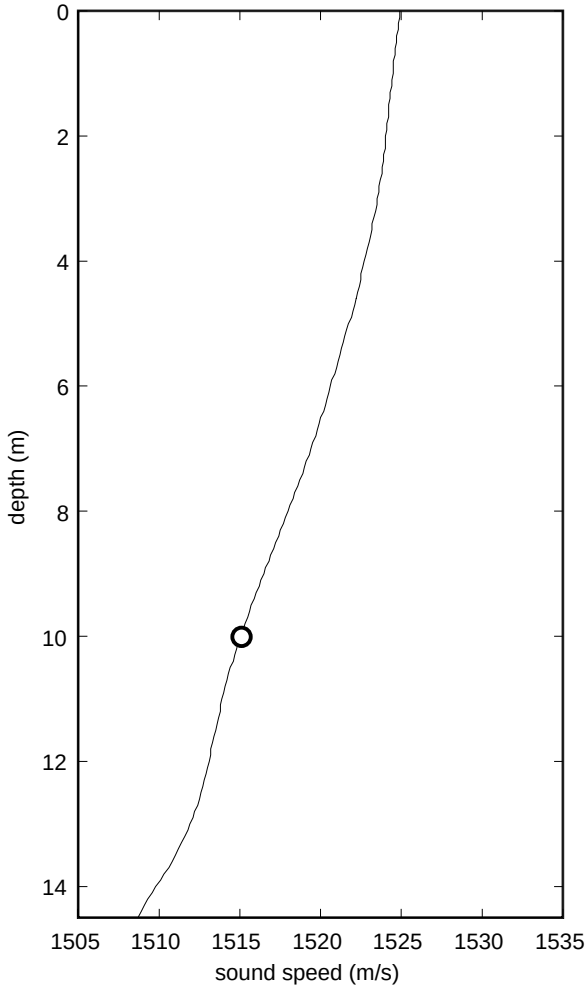

Fig. 7. Sound speed profile in water column, as measured during the experiment of 2 July 2002. The profile was determined from the average of four casts of a Sea-Bird temperature profiler, with smoothing applied using a curve-fitting routine. The small circle identifies the depth of the hydrophone that returned the spectrogram in Fig. 4(b).

7. Ray Structure in the Water Column

In a shallow water channel such as that sketched in Fig. 2, each of the propeller harmonics detected by a hydrophone will actually be a superposition of multipath arrivals. All such arrivals are refracted at the air-sea interface, of course, as illustrated in Fig. 8 for a direct and a first-bottom-bounce ray. In this example, both rays are shown with the same angle of elevation, that is, with identical Doppler shifts. To arrive at the receiver as shown, the first-bottom-bounce ray must be launched before the direct path ray, when the aircraft is further away from the sensor station. It should be evident that the overall multipath arrival structure is due, not just to rays launched from the aircraft at the angle shown in Fig. 8, but to all rays between the horizontal and vertical.

From the geometry shown in Fig. 8, it is straightforward to derive the reception time of a given ray as a function of elevation angle, θ_1, at the time of transmission. The result can be expressed as

$$t_{b,s} = \frac{h}{\sqrt{1-\cos^2\theta_1}}\left(\frac{1}{c_1} - \frac{\cos\,\theta_1}{v}\right) + \frac{2bd + (-1)^{b+s}z}{\sqrt{1-(c_2/c_1)^2\cos^2\theta_1}}\left(\frac{1}{c_2} - \frac{c_2}{c_1}\frac{\cos\,\theta_1}{v}\right), \qquad (5.1)$$

where d is the channel depth, z is the hydrophone depth and b, s are the numbers of bottom and surface bounces, respectively. Thus, for example, $t_{1,0}$ is the reception time of the first bottom bounce ray with no surface reflection. As before, the origin of time is taken to be when the aircraft is directly over the receiver. Now, as the angle of elevation, θ_1, is related

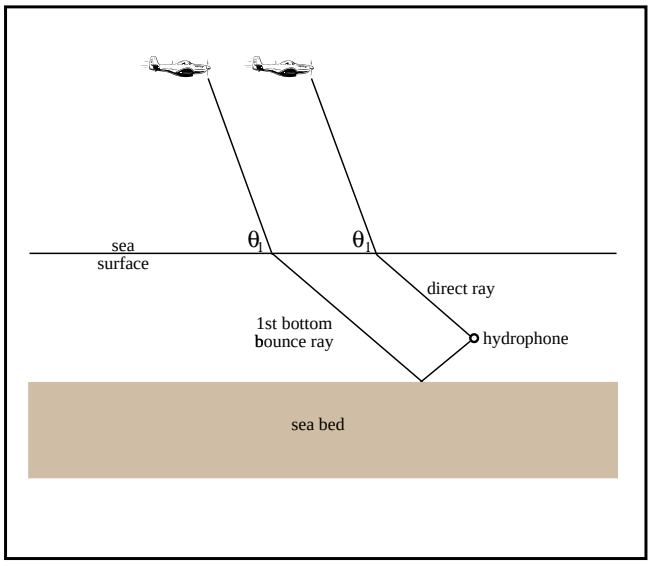

Fig. 8. Direct and first-bottom-bounce arrivals as the aircraft approaches a hydrophone, assuming total reflection at the sea bed. Both rays have the same launch angle and hence identical Doppler-shifted frequencies.

to the Doppler shifted frequency through Eq. (5.1),

$$f_D(\theta_1) = \frac{f}{1 - M\,\cos\,\theta_1}\,, \tag{5.2}$$

it is a simple matter to plot the time-frequency relationship of a given ray arrival at the hydrophone. Figure 9 is such a plot, showing the Doppler shifts of four rays as a function of time as the aircraft overflies the receiver station. The dashed regions of the curves involving a bottom reflection correspond to those angles of incidence at the sea bed which are less than the critical angle. Since most of the energy associated with these steep rays penetrates into the sediment, little arrives at the receiver in the water column.

Like a fast sea bed, the air-sea interface also shows a critical angle to acoustic energy incident from above. In this case, rays with an angle of elevation less than the critical grazing angle will be totally reflected (assuming a smooth sea surface) and accordingly will fail to reach a sub-surface receiver. This effect is not illustrated in Fig. 9 because it occurs at reception times that are well beyond those shown in the diagram. For instance, for the conditions of Fig. 9, the direct ray is totally reflected at the surface for reception times $|t_{0,0}| \geq 53.5$ s, corresponding to aircraft ranges in excess of 2.8 km; and the first bottom bounce ray is totally reflected by the sea surface at reception times $|t_{1,0}| \geq 193.1$ s, when the aircraft range exceeds 10.2 km. The corresponding numbers grow rapidly as the number of bottom and surface reflections increases.

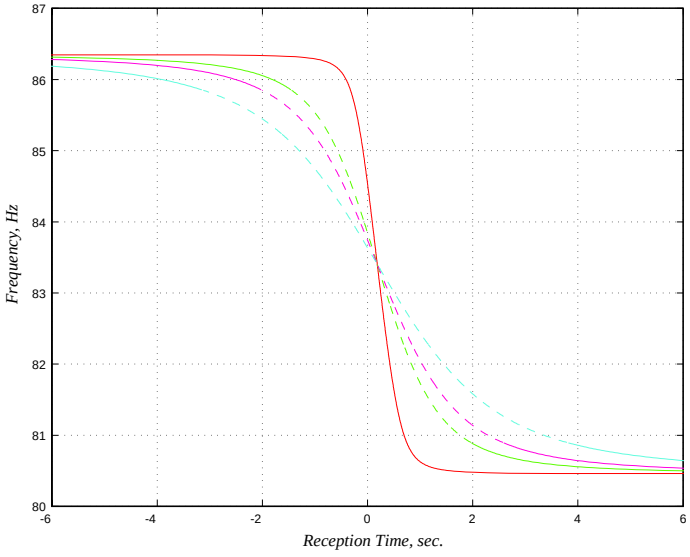

Fig. 9. Frequency-time plot from Eqs. (7.1) and (7.2) depicting four ray arrivals from the first propeller harmonic with intrinsic frequency of 83.3 Hz: direct ray (red), first bottom bounce (green), one bottom bounce and one surface reflection (magenta) and two bottom bounces with one surface reflection (cyan). The dashed regions indicate that the angle of incidence at bottom reflection is less than the critical angle and hence little energy from these steep rays arrives at the receiver. The parameters used in this example were: altitude $h = 66$ m, $v = 53$ m/s, $c_1 = 340$ m/s, $c_2 = 1500$ m/s, hydrophone depth $z = 10$ m and channel depth $d = 30$ m.

It is evident from Fig. 9 that it should be possible, with a vertical array of hydrophones, to steer a beam downwards to receive the upward-travelling, single bottom bounce arrival, whilst rejecting the downward-travelling direct and bottom-surface bounce rays. Those rays that suffer two or more bottom reflections are likely to be so attenuated as to be negligible at the receiver. According to this argument, a vertical array has the potential for isolating the single bottom bounce arrival, which, because it is modulated by the reflection coefficient of the bottom boundary, contains information about sediment properties, in particular the speed of sound in the granular medium. As a simple illustration of how bottom information could be extracted with the vertical array, consider that the time at which the single bottom bounce signal disappears from the arrival record is a direct measure of the critical angle of, and hence the sound speed in, the sediment. This technique, in which a vertical array is used to estimate the speed of sound in the sediment from the bottom reflection coefficient, is complementary to the method discussed earlier based on the Doppler difference frequency observed on a single buried sensor.

As pointed out above, the single bottom bounce signal could be present at the array when the range of the aircraft is within limits set by the critical angles of the sea surface and the sea bed. For the example of Fig. 9, this would place the aircraft between 160 m and 10.2 km. This suggests that it may be possible to use matched field techniques[25] on the data from an aircraft source and a vertical array of hydrophones to characterize the ocean environment.

8. Concluding Remarks

In underwater acoustics applications, light aircraft are unusual sources of sound, yet they would appear to have potential for obtaining information about the ocean environment, particularly the wave properties of the sea bed. An important consideration, of course, is whether sufficient acoustic energy from the aircraft penetrates the air-sea interface, and even into the sediment itself, to make inversion techniques possible. Our recent experiments off Scripps pier, in which acoustic sensors were placed in the atmosphere immediately above the sea surface, throughout the water column and in the sandy sediment, confirm that the sound from a low-flying, light aircraft is detectable in all three regions.

Calibrated spectra of the airborne, water-borne and sediment-borne sound signals from the aircraft, all show a well-defined harmonic structure, which is characteristic of propeller noise. Each harmonic exhibits a noticeable Doppler frequency shift, upwards as the aircraft approaches and downwards as it departs. The difference between the upward and downward shifted frequencies scales inversely with the local speed of sound, and hence is greatest in the slowest medium, that is, the atmosphere.

This inverse relationship between the Doppler difference frequency and the local speed of sound provides the basis of a simple technique for measuring the speed of sound in a marine sediment using a single, buried hydrophone. A second method of using an aircraft to infer sediment properties, from the bottom reflection coefficient, involves the coherent output of a vertical array of hydrophones in the water column as a means of separating

the single bottom bounce signal from other multipath arrivals. Obviously, the single buried phone technique has the advantage of requiring only one sensor but to some extent this is offset by the fact that a short line array of hydrophones in the water column is easier to deploy.

To date, five flying experiments have been performed off Scripps pier, which have yielded substantial, good quality acoustic data sets that are supported by the appropriate environmental (e.g. sound speed profiles in the water column) and navigational (e.g. GPS tracks of the aircraft) information. Most of the acoustic data have not yet been examined. What has been reported here represents a preliminary investigation of the acoustic records but is sufficient to indicate that the sound from a light aircraft is detectable in the air, the ocean and the sediment, and that the nature of the signals is such that an aircraft could be used as an acoustic source in ocean-acoustic inversion procedures. In fact, an elementary analysis of the Doppler data from the buried hydrophone yields an estimated speed of sound of 1617 m/s at a nominal frequency of 600 Hz in the very fine sand sediment approximately 1.5 km north-west of Scripps pier.

Acknowledgements

We are indebted to Dr. Michael D. Richardson, NRL, Stennis Space Center, for the loan of several shear sensors. Matthew B. Alkire provided assistance in analyzing the GPS data. This work was supported by Dr. J. Simmen, Ocean Acoustics Code, the Office of Naval Research, under grant number N00014-93-1-0054.

References

1. E. L. Hamilton, "Acoustic properties of sediments," in *Acoustics and the Ocean Bottom*, eds. A. Lara-Saenz, C. R. Cuierra, and C. Carbo-Fité (Consejo Superior de Investigacions Cientificas, Madrid, 1987), pp. 3–58.
2. M. D. Richardson, K. B. Briggs, D. L. Bibee *et al.*, *IEEE J. Oceanic Eng.* **26**(1), 26 (2001).
3. E. I. Thorsos, K. L. Williams, N. P. Chotiros *et al.*, *IEEE J. Oceanic Eng.* **26**(1), 4 (2001).
4. M. J. Buckingham and M. D. Richardson, *IEEE J. Oceanic Eng.* **27**(3), 429 (2002).
5. M. A. Biot, *J. Acoust. Soc. Am.* **28**, 168 (1956).
6. M. A. Biot, *J. Acoust. Soc. Am.* **28**, 179 (1956).
7. M. J. Buckingham, *J. Acoust. Soc. Am.* **108**, 2796 (2000).
8. A. B. Wood, *A Textbook of Sound*, 3rd ed. (G. Bell and Sons Ltd., London, 1964).
9. M. E. Goldstein, *Aeroacoustics* (McGraw-Hill, New York, 1976).
10. L. Gutin, Technical Memorandum Report No. NACA TM 1195, 1948.
11. A. A. Reigier and H. H. Hubbard, "Status of research on propeller noise and its reduction," *J. Acoust. Soc. Am.* **25**, 395 (1953).
12. M. J. T. Smith, *Aircraft Noise* (Cambridge University Press, Cambridge, 1989).
13. B. Magliozzi, D. B. Hanson, and R. K. Amiet, "Propeller and fan noise," in *Aeroacoustics of Flight Vehicles*, ed. H. H. Hubbard (Acoustical Society of America, Hampton, Virginia, 1995), Vol. 1, pp. 1-64.
14. D. G. Crighton, "Airframe Noise," in *Aeroacoustics of Flight Vehicles*, ed. H. H. Hubbard (Acoustical Society of America, Hampton, Virginia, 1995), Vol. 1, pp. 391-447.

15. R. J. Urick, *J. Acoust. Soc. Am.* **52**, 993 (1972).
16. W. J. Richardson, C. R. Greene Jr., C. I. Malme, and D. H. Thomson, *Marine Mammals and Noise* (Academic Press, New York, 1995).
17. H. Medwin, R. A. Helbeig, and J. D. Hagy Jr., *J. Acoust. Soc. Am.* **54**, 99 (1973).
18. M. J. Lighthill, *Waves in Fluids* (Cambridge University Press, 1978).
19. A. D. Pierce, *Acoustics: An Introduction to its Physical Principals and Applications* (McGraw-Hill, New York, 1981).
20. M. J. Buckingham, *J. Acoust. Soc. Am.* **102**, 2579 (1997).
21. E. L. Hamilton, *J. Geophys. Res.* **75**(23), 4423 (1970).
22. E. L. Hamilton, *Geophys.* **37**(4), 620 (1972).
23. M. D. Richardson, "Spatial variability of surficial shallow water sediment geoacoustic properties," in *Ocean-Seismo Acoustics: Low-Frequency Underwater Acoustics*, eds. T. Akal and J. M. Berkson (Plenum, New York, 1986), pp. 527–536.
24. M. D. Richardson and K. B. Briggs, "On the use of acoustic impedance values to determine sediment properties," in *Acoustic Classification and Mapping of the Seabed*, eds. N. G. Pace and D. N. Langhorne (University of Bath, Bath, 1993), Vol. 15, pp. 15–24.
25. A. Tolstoy, *Matched Field Processing for Underwater Acoustics* (World Scientific, Singapore, 1993).